JOURNAL OF SPACECRAFT AND ROCKETS
Vol. 46, No. 1, January–February 2009

Experimental Investigation of a Passive Deployable/Stowable Radiator

Hosei Nagano,* Akira Ohnishi,† and Ken Higuchi‡
Japan Aerospace Exploration Agency, Sagamihara, Kanagawa 229-8510, Japan
and
Yuji Nagasaka§
Keio University, Yokohama, Kanagawa 223-8522, Japan

DOI: 10.2514/1.30170

A passive deployable/stowable radiator, reversible thermal panel has been developed for thermal control of interplanetary spacecrafts. The reversible thermal panel can autonomously adapt to a wide variety of thermal environments with no electrical power. A reversible thermal panel prototype model was fabricated and extensive test programs including fin deployment/stowing tests, thermal performance tests, and vibration tests have been executed to validate that the reversible thermal panel prototype model can meet all the qualification requirements. Deployment/stowing tests have demonstrated repeatable reversible thermal panel fins deploy/stow from 0 to 140° over the temperature range from −30 to +30°C. Thermal performance tests, including thermal balance tests and power cycling tests, have shown reversible thermal panel's autonomous thermal control for changes in thermal conditions. The reversible thermal panel has also been subjected to qualification-level vibration loads and passed with no significant issues.

I. Introduction

TO ADJUST the spacecraft temperature to a wide variety of thermal environments for future space missions, it is indispensable to establish the heat switch technologies such as thermal louver, variable emittance coatings, and paraffin actuator [1–4]. Japan Aerospace Exploration Agency/Institute of Space and Astronautical Science (JAXA/ISAS) has developed a lightweight 100-W-class redeployable radiator with environment-adaptive functions as an approach. This radiator, reversible thermal panel (RTP), has been investigated for applications where a wider variation of thermal performance and high heat dissipation are required. RTP consists of a baseplate, flexible high-thermal-conductivity materials, and a passive reversible actuator [5,6]. RTP is a conductive deployable radiator which allows for the optional addition of dual functions, one of which changes the radiator fin angle according to the inner temperature of the spacecraft, and also serves as a solar absorber that absorbs solar energy for heat retention of electronics. When the internal temperature increases due to the change of the total amount of heat load or external thermal environment, the actuator increases its torque as well. This, in turn, generates forces that rotate the reversible fin toward its deployed position, leading to an increase in radiation into space. As the temperature decreases, however, the actuator moves the reversible fin toward its stowed position, completely covering the surface of the baseplate radiator with the radiator side of the reversible fin, and blocks more of the radiator's exposure to space. In addition, if solar irradiation is available, solar power is absorbed and used as a heat source for the survival heater. That is, the RTP absorber surface absorbs the sunlight and converts it into heat that is transported into the heat source and warms it. This autonomous deployment and stowing of the reversible fin maintains acceptable temperatures by compensating for changes in dissipation and environment heating.

The RTP development has been in operation since 2002, and its feasibility has been experimentally demonstrated [5]. The RTP is considered as one of the candidates of thermal control methodology for the Japanese Venus mission "Planet-C" which will be launched in 2010 by an H-IIA rocket developed by JAXA [7]. In this mission, a small spacecraft weighing approximately 500 kg will enter orbit around Venus after 12 months orbiting around Earth. One major problem to solve is how much survival heater power can be saved in the Earth's orbit because the solar intensity around Venus is about twice as high as that around Earth. The RTP can be a good solution to the problem. Development of an RTP prototype model (PM), which was designed based on the detailed thermal and structural analyses, has been ongoing since 2005 with the criteria that 1) the device is thermally and structurally consistent as a spacecraft application and 2) it can satisfy the requirements of the Venus mission [8].

This paper describes the test results of an extensive test program, which has been executed for the RTP-PM to validate the former subject. The tests performed for qualification are as follows: 1) fin deployment/stowing tests, 2) thermal performance tests, and 3) vibration tests.

The deployment/stowing tests were conducted to demonstrate the actuator performance of the fin deploy/stow against the change of the actuator temperature. The thermal performance tests were performed 1) to evaluate the RTP basic thermal performance, 2) to demonstrate the autonomous thermal control function, and 3) to validate reliable repeatability of the RTP performance in cycling thermal conditions in a simulated space environment. The vibration tests were conducted to validate the RTP structural integrity in the launch random vibration environment. Vibration testing includes random vibration testing and sine vibration testing subjected to the H-IIA launch vehicles specification.

II. Reversible Thermal Panel Hardware Design Description

Figure 1 illustrates the RTP-PM, which is composed of a baseplate, heat transport units, surface material, a passive reversible actuator (RA), a hold and release mechanism (HRM), support, and

Presented as Paper 1215 at the 45th AIAA Aerospace Sciences Meeting and Exhibit, Reno, Nevada, 8–11 January 2007; received 27 March 2007; accepted for publication 22 October 2007.

*Researcher, Institute of Space and Astronautical Science, Department of Space Structure and Materials Engineering, 3-1-1 Yoshinodai. Member AIAA.

†Assistant Professor, Institute of Space and Astronautical Science, Space Expulsion Engineering Department, 3-1-1 Yoshinodai.

‡Associate Professor, Institute of Space and Astronautical Science, Department of Space Structure and Materials Engineering, 3-1-1 Yoshinodai.

§Professor, Department of System Design Engineering, 3-14-1 Hiyoshi.

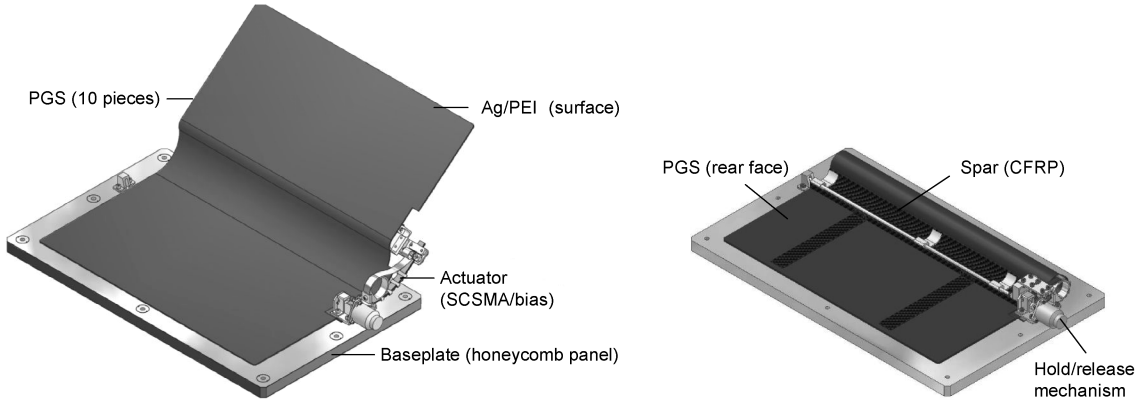

a) Deployed b) Stowed

Fig. 1 RTP prototype model.

rods. The materials and sizes of these items are listed in Table 1. The heat transport unit is composed of a flexible thermal conductive material and nonwoven copper fabric. A pyrolytic graphite sheet (PGS) was selected as a flexible thermal conductive material.

RTP-PM configurations such as dimensions, fin thickness, and aspect ratio are almost the same as that of the RTP engineering model (EM) which was optimized based on weight and thermal performance [5]. The following modifications were made for the RTP spaceflight hardware [6]:

1) A portion of the heat transport unit is attached on the top of the baseplate for easy installation, whereas previously it was attached between the bottom of the baseplate and equipment in the EM.

2) A new RA based on the new deployment/stowing mechanism with a new material was developed.

3) Nonwoven copper fabric was installed in the heat transport unit to reinforce PGS lamination.

4) A hold and release mechanism was attached to ensure non-deployment of the RTP fin under a launch vibration environment. Structural support parts were also added.

Figure 2 shows the composition of the heat transport unit. Ten layers of PGS and two nonwoven copper fabrics were laminated with sheet adhesives. Nonwoven copper fabrics were installed to reinforce the PGS due to frailness. Figure 3 is a photograph of a PGS laminated fin to which the nonwoven copper fabrics were attached. Silverized polyester imide film (Ag/PEI) with a low solar absorptance to the infrared-emittance ratio (α_S/ε_H) was added on the surfaces of the radiator for heat dissipation, though no surface material was attached to the PGS absorber fin. Thermal conductivity and optical properties of the PGS were reported in [9–11].

Figure 4 shows the passive RA, which consists of a single crystal shape memory alloy (SCSMA) leaf spring, a bias spring which provides a constant torque, and a support cylinder. SCSMA is a new material currently under development at TiNi Aerospace with a transformation temperature range from −270 to +180°C. The SCSMA has about 3 times grater strain recovery than that of conventional SMAs. Force balance between the SCSMA and the bias spring of the actuator determines the fin deployment angle. When the SCSMA reaches its transition temperature, it generates a shape recovery force that deploys the reversible fin. As the temperature decreases, the force of the bias spring becomes dominant and the actuator moves the fin toward its stowed position. The RA is insulated by a foam insulation and a multilayer insulation (MLI) to minimize heat exchange with external thermal environments. In its initial condition, the RTP was mechanically fixed by the HRM which is released in orbit for the purpose of protecting the RTP parts from the intense acoustic environment and vibration during the launch phase of the mission. HRM is connected with a stiffening rod and the

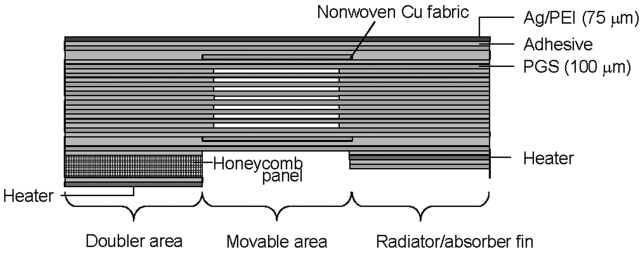

Fig. 2 Cross-sectional view of heat transport unit (not to scale).

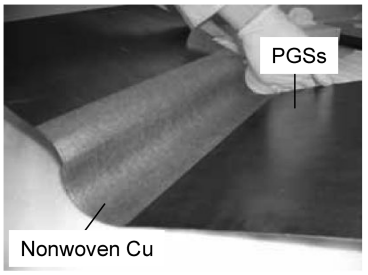

Fig. 3 Photograph of PGS lamination with nonwoven copper fabrics.

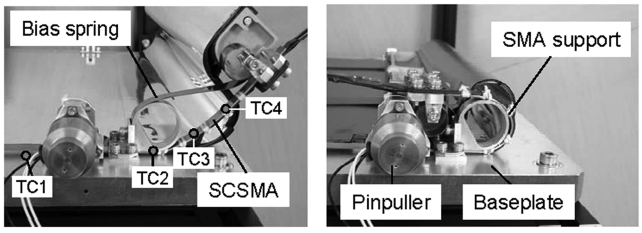

a) Deployed b) Stowed

Fig. 4 Photographs of reversible actuator.

Table 1 RTP specification

Component	Material	Size & mass
Radiator fin	PGS nonwoven Cu Ag/PEI (surface)	180 × 500 × 1 mm, 180 g
Reversible actuator	SCSMA/bias spring SMA support	35 g
Hold/release mechanism	Pinpuller rod	90 g
Spar and rib	CFRP polyimide shape	33 g
Baseplate	A2024 (0.3 mm × 2,) Al 1/4-5052-0.01P-t14	410 × 200 mm, 347 g
Total mass	(Including baseplate), (excluding baseplate)	685 g, 338 g

rib with a carbon fiber reinforced plastic (CFRP) which is attached to the RTP fin.

III. Deployment/Stowing Tests

Fin deployment/stowing tests were performed in an atmospheric condition to verify the deployment/stowing performance of the RTP actuator as a function of its temperature. It was analytically proven that when the deployment fin angle is 120 deg, the heat-rejection performance is about 98% of the heat-rejection performance during full fin deployal [5]. Therefore, it is critical that the fin deployment angle under the new actuator is more than 120 deg.

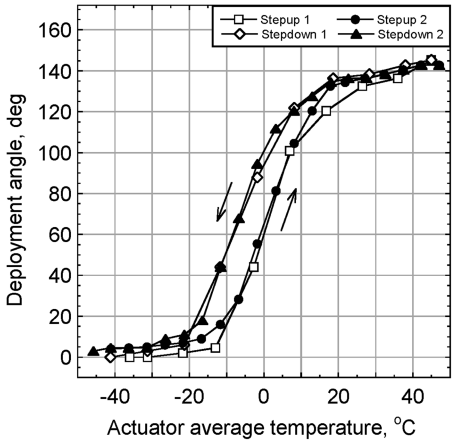

Fig. 5 Fin deployment angle as a function of actuator temperature.

A. Test Setup

The RTP was set vertically in a constant temperature chamber so that the actuator was positioned at the very top of the RTP. The temperature of the chamber was controlled to a range of −45– + 45°C. Four thermocouples were attached to the SCSMA to monitor the temperature distribution as indicated in Fig. 4a. When the actuator temperature reached steady state, the fin deployment angle was measured by a protractor which was equipped above the actuator. At first, the temperature of the chamber was set around −45°C. The temperature was then increased to +45°C (stepup), and finally reduced from +45°C to −45°C (stepdown). This test was repeated twice. The ratio of rising/decreasing temperature in the constant temperature chamber was 5:10°C.

B. Deployment/Stowing Test Results

Figure 5 presents the fin angle of the RTP as a function of actuator average temperature. The temperature distribution among the actuator measured by the four thermocouples was less than ±0.2°C. In these two tests, similar characteristics could be obtained although there was a slight difference in the track of the temperature-angle

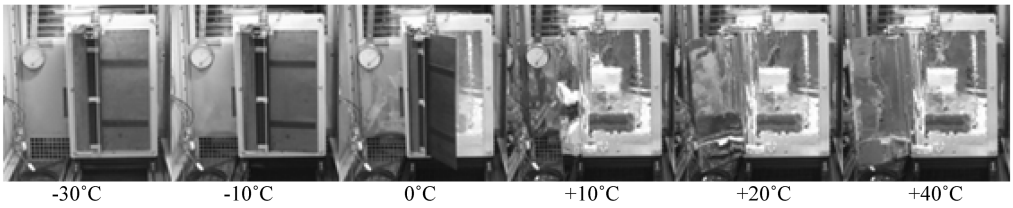

a) Stepup

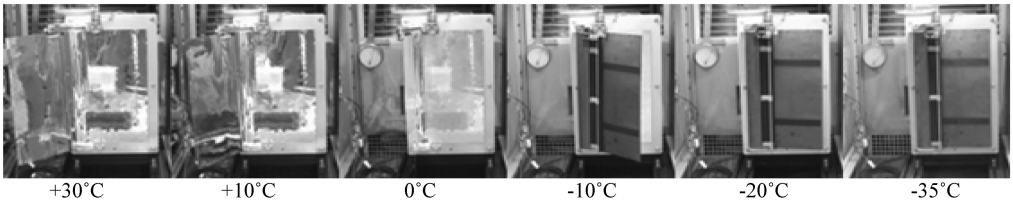

b) Stepdown

Fig. 6 Photographs of RTP-PM in deployment/stowing tests.

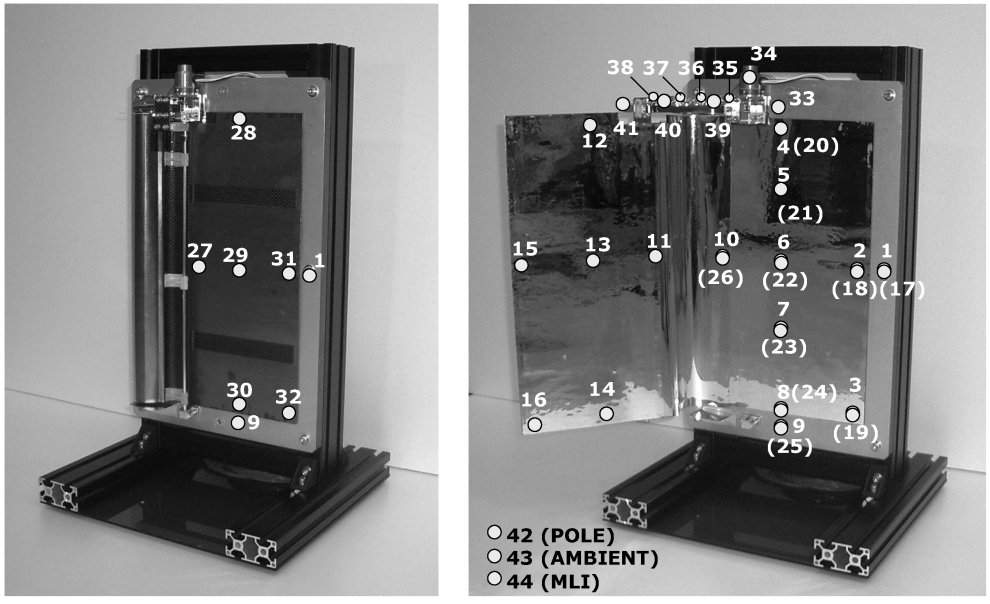

Fig. 7 Thermocouple locations on the RTP-PM (parentheses indicate the rear side).

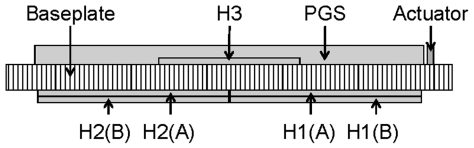

Fig. 8 Heater locations on the RTP-PM (cross-sectional view).

curve. In the temperature step-up process, the fin started opening around −10°C and reached 120 deg deployment at about 20°C. At 30°C, the fin deployment angle reached almost the maximum of 140 deg. In the step-down process, the fin started closing around 10°C, the fin deployment angle was about 15 deg at −20°C, and the fin was almost entirely stowed at −30°C. The test results show that the actuator can reversibly change the fin angle from 0 to 140 deg. About a 10°C temperature hysteresis, which was the nature of the SCSMA characteristics, between the heating and cooling processes was observed. Figure 6 shows the photographs of the RTP at various temperatures in the deployment/stowing tests.

IV. Thermal Performance Tests

After the deployment/stowing test, a thermal balance test and a thermal cycling test were conducted in a vacuum condition. The purposes of these tests are 1) to evaluate the RTP basic thermal performance, 2) to demonstrate the autonomous thermal control function, and 3) to validate the repeatability of the RTP performance in cycling thermal conditions in a simulated space environment.

A. Test Setup and Test Conditions

Figure 7 indicates thermocouple locations on the RTP-PM. Forty T-type (200 μm) thermocouples were used to measure the RTP's overall temperature. Four K-type (50 μm) thermocouples were attached on the SCSMA for thermal distribution measurement. Four sheet heaters were attached on the baseplate to simulate heat inputs from the equipment. One sheet heater was attached to the absorber fin to simulate solar irradiation. The location of the heaters on the RTP is depicted in Fig. 8. Three different heat loads were applied on the RTP base plate and the RTP absorber fin as listed in Table 2. The purpose of the heat input variation is to evaluate the RTP performance in low heat flux mode (LHX) and high heat flux mode (HHX) and to evaluate the solar absorptive function of the RTP [solar heat input (SHI) mode]. The RTP was fixed at a support flame by means of glass-epoxy spacers and polycarbonate bolts. With the exception of the radiator surface of the baseplate and the deployable/stowable fin, that is, edges and rear side of the baseplate were covered and insulated by seven layers of thermal blanket. Because there was a slight space for radiation from the radiator surface even when the fin was entirely stowed, shades were attached around the rotary axis.

Table 2 Heat input mode

Mode	Heaters used	Resistance
LHX	H1(A) + H2(A)	25.6 Ω
HHX	H1(A) + H1(B)	25.6 Ω
SHI	H3	23.3 Ω

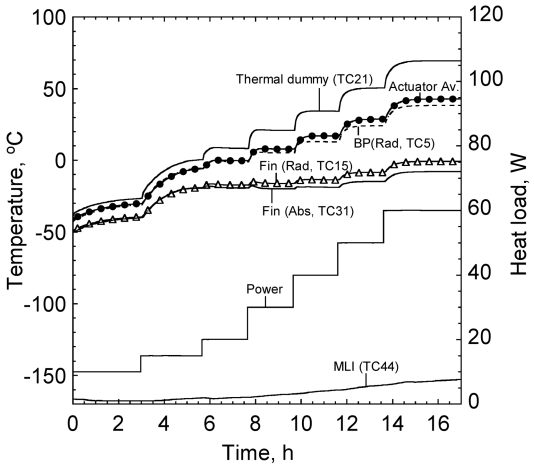

Fig. 9 Temperature profile during autonomous thermal control test (stepup).

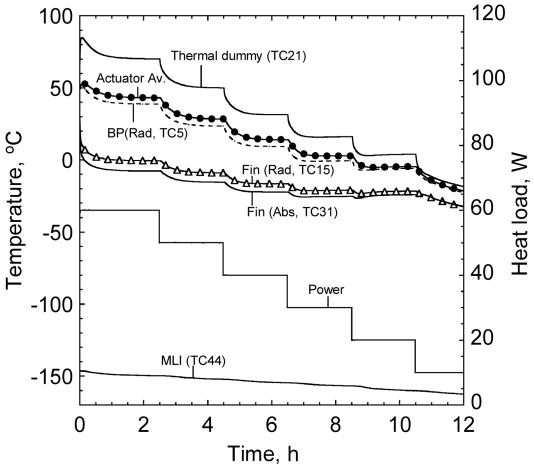

Fig. 10 Temperature profile during autonomous thermal control test (stepdown).

Table 3 lists all tests performed in a vacuum condition. The purpose of an autonomous thermal control test was to evaluate the heat-rejection capability and the corresponding supplied heater power on the thermal dummies (TD), which simulate the heat input from electric equipments. The TD heaters were set to an input wattage of 5–70 W. The power cycling test was conducted to evaluate the repeatability of the RTP autonomous control. The temperatures of the RTP were recorded throughout the entire test at 3-min intervals. Detailed descriptions of the test system can be found in the literature [7].

Table 3 Test conditions

Tests	Launch lock	Heat input mode	Applied power	No.
Solar absorption	On	SHI	35 W/30 W/25 W/20 W/15 W/10 W/	1
Retention	On	LHX	10 W/20 W/30 W	2
		HHX	20 W/10 W/7.5 W	3
Lock release	On → Off	HHX	7.5 W to the heater, 9.5 W was applied to the pinpuller	4
Autonomous thermal control	Off	LHX	10 W/15 W/20 W/30 W/40 W/50 W/60 W/70 W/80 W (stepup)	5
			70 W/60 W/50 W/40 W/30 W/20 W/10 W (stepdown)	6
		HHX	10 W/15 W/20 W/30 W/40 W/50 W/60 W (stepup)	7
			60 W/50 W/40 W/30 W/20 W/10 W (stepdown)	8
Power cycle	Off	LHX	40 W/60 W/20 W/60 W/20 W/40 W	9
			60 W/10 W/60 W/20 W/60 W/30 W/60 W/0 W/60 W	10
		HHX	40 W/50 W/15 W/60 W/15 W/30 W/15 W/40 W/15 W/50 W/15 W	11

B. Thermal Performance Test Results

1. Autonomous Thermal Control Tests

Figures 9 and 10 illustrate the temperatures of the front and back of the baseplate (TC5 and TC21), the tips of the radiator (Rad, TC15) and absorber fins (Abs, TC31), the MLI (TC44), and the actuator (average of TC35-38, Av) in the autonomous thermal control test during power stepup and stepdown in HHX mode (tests 7 and 8). At 20 W application in Fig. 9, the temperature suddenly stopped increasing. From this point, the fin began to deploy. From 20 to 50 W, the fin deployment angle was passively controlled and balanced as evidence that the fin temperature stayed almost constant. From 40 to 20 W in Fig. 10, a similar tendency can be seen. The temperature difference between the thermal dummy and the tip of the fin (radiator side) in 60 W power application was about 69°C.

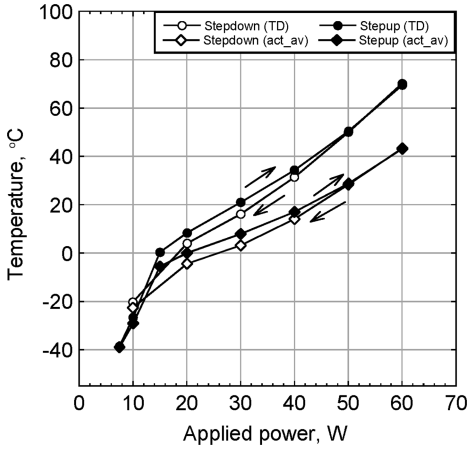

Fig. 11 Temperature of the RTP thermal dummy and actuator average as a function of applied power.

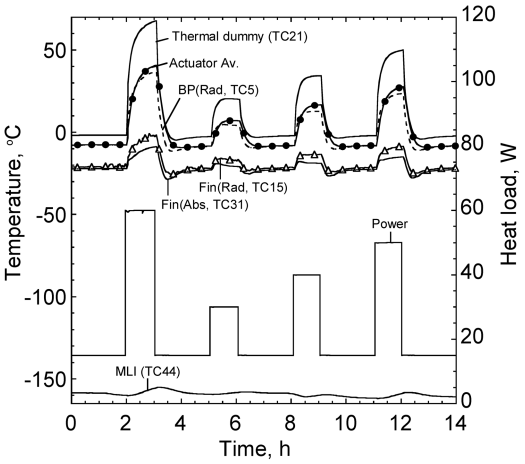

Fig. 12 Temperature profile during power cycling test.

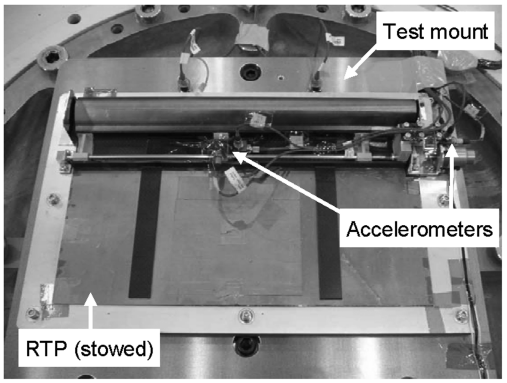

Fig. 13 Photograph of test setup for *Z*-axis vibration testing.

Table 4 Vibration tests spectrum

Tests	Frequency	Specification
Random	20–2000 Hz	Overall 10.4 Grms (80 s) (*X* axis) Overall 10.4 Grms (80 s) (*Y* axis) Overall 17.0 Grms (80 s) (*Z* axis)
Sine	5–100 Hz	25 G (all axes)

Figure 11 presents the temperature at the hottest point of the thermal dummy and the actuator average temperature as a function of the applied power to the RTP in HHX mode. It was confirmed that the fin could change the deployment angle autonomously along with the heat load. Because of this deployment during the step-up process, the actuator temperature increased as the heat load increased, and the SCSMA generated force and deployed the RTP fin. In the step-down process, the opposite scenario can be applied. By autonomous deployment/stowing of the fin, the temperature change of the RTP thermal dummy with the change of the heat load was moderate. The temperature difference between the thermal dummy and the actuator was about 27°C on average.

2. Power Cycling Tests

Three kinds of power cycling tests were conducted. Power was applied so that the temperature of the SCSMA, which is a part of the actuator, went across the phases among austenite, martensite, and their intermediate phase. Figure 12 gives an example of a power cycle test in HHX mode (part of test 11). In this test, the power of 15 W was initially applied to the RTP and the RTP had reached steady state. Power application to the heater was suddenly increased to different power levels (60, 30, 40, and 50 W) for 1 h and then reduced to 15 W again for 2 h. These cycles were repeated 4 times. It was confirmed that there were several bumps in the temperature change, especially when the power was reduced from high power to 15 W. At these points, it is considered that the RA stowed the RTP fin along with the changes in temperatures and, as a result, the sudden falls of the thermal dummy temperature were moderated. Overall temperature distribution when the 15 W was applied shows almost the same temperature as the same power application after a power cycle. This indicates that there is no degradation of the actuator caused by the heat cycle. In total, more than 10 power cycles were applied to the RTP, and good repeatability of the temperature was shown.

V. Vibration Tests

Vibration testing was performed after the thermal performance test. Vibration testing includes random vibration testing and sine vibration testing, the specification of which is based upon the H-IIA launch vehicle by which the Planet-C will be launched.

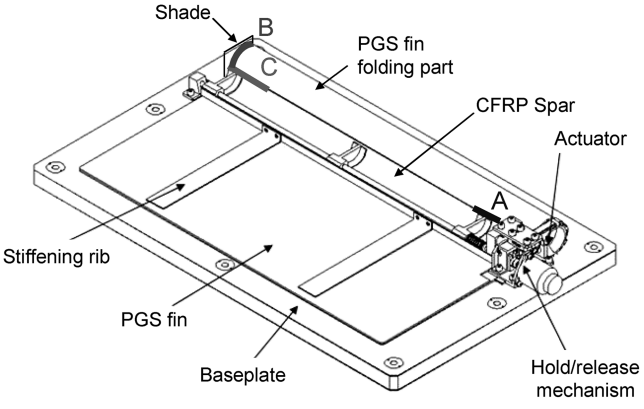

Fig. 14 Location of minor damaged part.

Table 5 Detailed description of issues that occurred and action items

No.	Issues	Action items for the future
1	There was initially a slight crack between the outer layer of the PGS fin folding part and the CFRP spar at location A in Fig. 14. The crack got larger due to the vibration of the PGS fin folding part.	Because it is just the damage of the outer layer of the PGS fin, no critical effects on thermal performance were observed. Nonwoven copper fabric should be installed to avoid this issue.
2	The shade vibrated during the test, and the shade hit the fold edge of the PGS fin at location B in Fig. 14. The tip of the PGS fin suffered minor damage.	Much clearance between shade and PGS fin will be prepared, or the shade will be strengthened against the vibration.
3	The CFRP spar which was attached to the PGS fin at location C was partially removed due to the peeling off of the outer layer of the PGS fin folding part during vibration.	Nonwoven copper fabric should be installed to avoid this issue.

A. Test Setup and Test Performed

The test assembly was instrumented with a total of six triaxial response accelerometers for vibration response measurement. Four of those were located on the vibration test mounts while two were located on the RTP as shown in Fig. 13. All accelerometers were bonded directly to the test article and additionally restrained by Kapton tape. Vibration testing was performed in the JAXA/ISAS. A photograph of the RTP-PM in its final configuration for Z-axis excitation is shown in Fig. 13.

The qualification test level specification, shown in Table 4, has a total level of 10.4 Grms in X and Y orthogonal axes and 17.0 Grms in the Z axis for a duration of 80 s per axis. Before and after the qualification-level random vibration tests and sine vibration tests, random vibration tests at a level of -12 dB were done to monitor the resonance frequencies and to verify structural integrity. Vibration testing in the lateral directions (X and Y axes) were performed first. After the X and Y axes testing was completed, the test assembly was moved to the medium vibration test facility and configured for vertical excitation. The same test sequence was then repeated for the Z axis. After each test, a visible inspection was performed. In addition to that, after all vibration testing was completed, the RTP was disassembled and a detailed inspection, a launch–lock release test, and a deployment/stowing test were performed.

B. Vibration Test Results

Random vibration testing, at the specified vibration spectrum, was successfully performed and completed for all three axes. There was little difference in the data of -12 dB pre- and post-tests of random vibration tests and sine vibration tests. After testing was completed, the RTP was disassembled and inspected. There was some minor visible damage to the RTP. Figure 14 depicts the damaged part and Table 5 lists a detailed description of issues that occurred. They are not expected to have an effect on the structural integrity of the RTP. Other than this, there was no visible damage to any portion of the RTP. The launch–lock release test and the deployment/stowing test were conducted after the vibration tests. These systems worked properly as they did before the vibration testing.

VI. Conclusions

RTP-PM was developed and three tests, such as 1) deployment/stowing tests, 2) thermal performance tests, and 3) vibration tests, were conducted to validate that the RTP-PM can meet the qualification requirements. The fin deployment/stowing tests have demonstrated repeatable RTP fins that deploy/stow from 0 to 140 deg over the actuator temperature range of -30 to $+30$°C. Thermal performance tests including thermal balance tests and power cycling tests have showed RTP's autonomous thermal control with the change of various power levels. Although the vibration test results induced minor visible damages to the RTP-PM, they are not expected to have an effect on the structural integrity of the thermal control subsystem. Based on the successful vibration testing and performance testing, the RTP-PM has been demonstrated to be of flight quality.

Acknowledgments

The authors are grateful to the Planet-C project group at the Japan Aerospace Exploration Agency/Institute of Space and Astronautical Science (JAXA/ISAS) for its financial support. The authors also would like to express their appreciation to Kazuki Watanabe and Yu Oikawa of the WEL Research Co., Ltd, and to Nobukatsu Okuizumi and Kyoichi Ui of ISAS for assisting with the vibration testing.

References

[1] Osiander, R., Champion, J. L., Darrin, A. M., Sniegowski, J. J., Rodgers, S. M., Douglas, D., and Swanson, T. D., "Micromachined Louver Arrays for Spacecraft Thermal Control Radiators," AIAA Paper AIAA-2001-0215, 2001.

[2] Pauken, M., Sunada, E., Novak, K., Phillips, C., Birur, G., and Lankford, K., "Development Testing of a Paraffin-Actuated Heat Switch for Mars Rover Applications," Society of Automotive Engineers (SAE) Paper 2002-01-2273, 2001.

[3] Tachikawa, S., Ohnishi, A., Shimakawa, Y., Ochi, A., Okamoto, A., and Nakamura, Y., "Development of a Variable Emittance Radiator Based on a Perovskite Manganese Oxide," *Journal of Thermophysics and Heat Transfer*, Vol. 17, No. 2, 2003, pp. 264–268. doi:10.2514/2.6760

[4] Braig, A., Meisel, T., Rothmund, W., and Braun, R., "Electro Emissive Devices—Progress Made in Development," Society of Automotive Engineers (SAE) Paper 941465, 1994.

[5] Nagano, H., Ohnishi, A., and Nagasaka, Y., "Development of a Flexible Thermal Control Device with High-Thermal-Conductivity Graphite Sheets," Society of Automotive Engineers (SAE) Paper 2003-01-2471, 2003.

[6] Nagano, H., Nagasaka, Y., and Ohnishi, A., "Simple Deployable Radiator with Autonomous Thermal Control Function," *Journal of Thermophysics and Heat Transfer*, Vol. 20, No. 4, 2006, pp. 856–864. doi:10.2514/1.17988

[7] Nakamura, M., Imamura, T., Ueno, M., Iwagami, N., Satoh, T., Watanabe, S., Taguchi, M., Takahashi, Y., Suzuki, M., Abe, T., Hashimoto, G., Sakanoi, T., Okano, S., Kasaba, Y., Yoshida, J., Yamada, M., Ishii, N., Yamada, T., Uemizu, K., Fukuhara, T., and Oyama, K., "Planet-C: Venus Climate Orbiter mission of Japan," *Planetary and Space Science*, Vol. 55, No. 12, 2007, pp. 1831–1842. doi:10.1016/j.pss.2007.01.009

[8] Nagano, H., Nagasaka, Y., Ohnishi, A., Watanabe, K., Oikawa, Y., and Yamaguchi, K., "Design and Fabrication of a Passive Deployable/Stowable Radiator," Society of Automotive Engineers (SAE) Paper 2006-01-2038, 2006.

[9] Nagano, H., Kato, H., Ohnishi, A., and Nagasaka, Y., "Measurement of Thermal Diffusivity of Anisotropy Graphite Sheet Using AC Calorimetric Method," *International Journal of Thermophysics*, Vol. 22, No. 1, 2001, pp. 301–312. doi:10.1023/A:1006780208048

[10] Nagano, H., Ohnishi, A., and Nagasaka, Y., "Thermophysical Properties of High-Thermal-Conductivity Graphite Sheets for Spacecraft Thermal Design," *Journal of Thermophysics and Heat Transfer*, Vol. 15, No. 3, 2001, pp. 347–353. doi:10.2514/2.6614

[11] Nagano, H., Ohnishi, A., Nagasaka, Y., Mori, Y. H., and Nagashima, A., "Proton Irradiation Effects on Thermophysical Properties of High-Thermal-Conductive Graphite Sheet for Spacecraft Application," *International Journal of Thermophysics*, Vol. 27, No. 1, 2006, pp. 114–125. doi:10.1007/s10765-006-0017-6

J. Olejniczak
Associate Editor